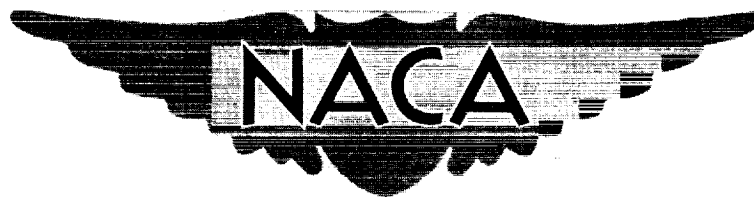


# CASE FILE COPY



## RESEARCH MEMORANDUM

STABILITY OF BODIES OF REVOLUTION HAVING FINENESS

RATIOS SMALLER THAN 1.0 AND HAVING

ROUNDED FRONTS AND BLUNT BASES

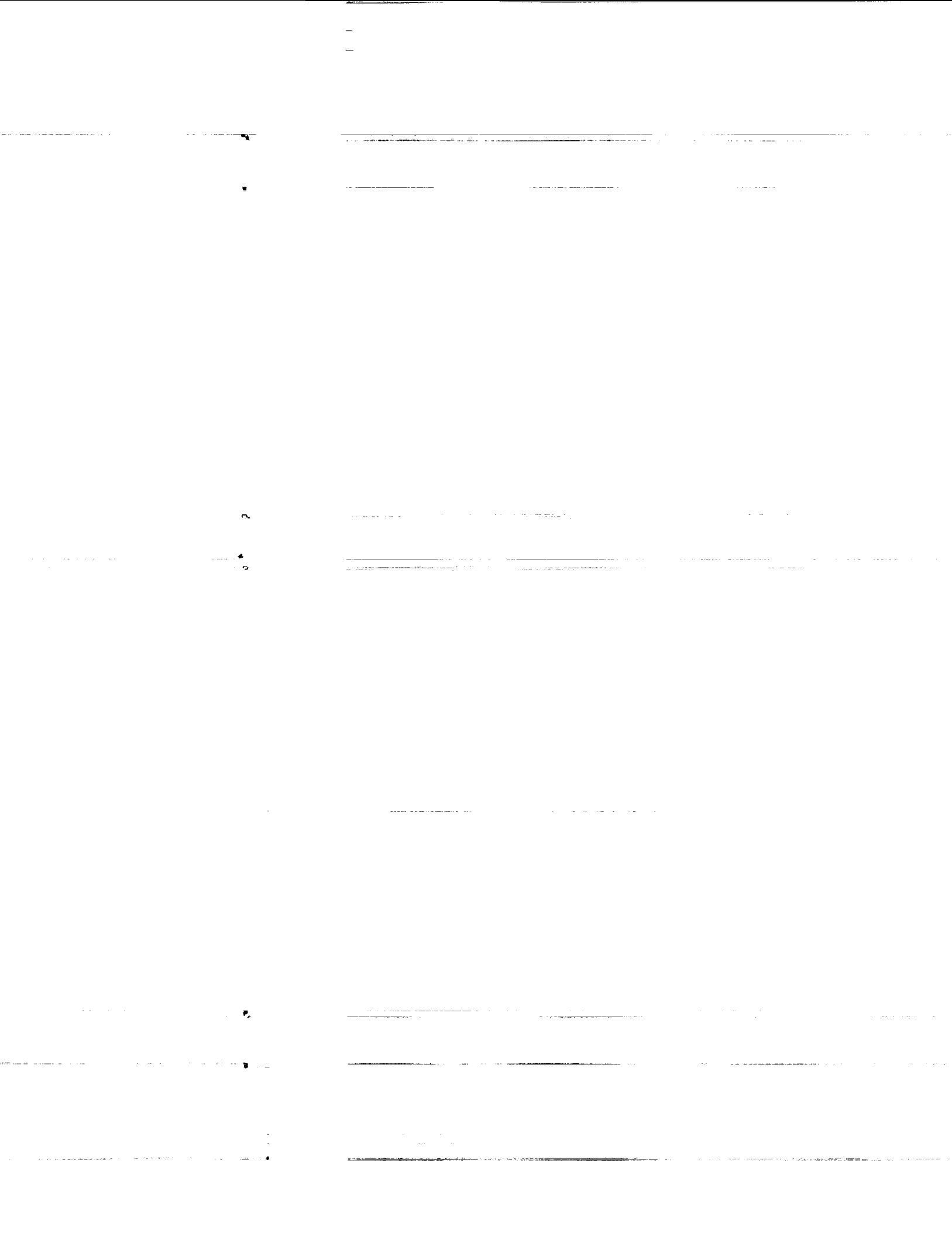
By Stanley H. Scher and James S. Bowman, Jr.

Langley Aeronautical Laboratory  
Langley Field, Va.

NATIONAL ADVISORY COMMITTEE  
FOR AERONAUTICS

WASHINGTON

January 29, 1953  
Declassified December 13, 1957



## NATIONAL ADVISORY COMMITTEE FOR AERONAUTICS

## RESEARCH MEMORANDUM

STABILITY OF BODIES OF REVOLUTION HAVING FINENESS  
RATIOS SMALLER THAN 1.0 AND HAVING  
ROUNDED FRONTS AND BLUNT BASES

By Stanley H. Scher and James S. Bowman, Jr.

## SUMMARY

An investigation has been made of the stability of several bodies of revolution having fineness ratios smaller than 1.0 and having rounded fronts and blunt bases. Free-drop tests were made in the vertical Langley 20-foot free-spinning tunnel to determine the behavior of the various bodies in descent. The results indicated that the stability of the bodies as determined from observed motions decreased as the body shapes varied from a hemisphere to a near-paraboloid. Free-oscillation tests were made for some of the bodies and the static stability parameter  $C_{m\alpha}$  was found to be indicative of the relative behaviors noted during the free-drop tests. In addition to the determination of stability from the free-body tests, a method for calculating the approximate stability of the subject type of body was developed. Results obtained by this calculation method agreed well with the experimental results.

## INTRODUCTION

Recently, interest has been expressed in the behavior in descent of various bodies of revolution with rounded fronts and blunt bases and with fineness ratios less than 1.0. Inasmuch as the theories, such as those presented in references 1 and 2, which are available for calculating the stability of bodies of revolution are not applicable to bodies of such small fineness ratio, experimental free-drop tests to determine the inherent behavior of several such bodies have been made. The tests were made in the vertical air stream of the Langley 20-foot free-spinning tunnel, and the body shapes included a hemisphere, a near-paraboloid, and four intermediate bodies. Some of the bodies (those which were stable), while free in the air stream, were oscillated in a single plane and their degrees of stability were determined from observed damping times and periods of the oscillations. In addition, a method for calculating

the approximate static stability of the subject types of bodies is developed and applied to the bodies.

### SYMBOLS

x	axial distance from bow of body to any body station
r	local body radius at any station x
L	body length
$I_y$	moment of inertia about lateral body axis through center of gravity perpendicular to longitudinal body axis
V	free-stream velocity
$\alpha$	angle of attack (body-axis inclination relative to free-stream flow direction)
$C_{D_{\alpha=0^\circ}}$	drag coefficient of body at an angle of attack of $0^\circ$ , $\frac{\text{Weight}}{qS}$
S	area of base of body
q	free-stream dynamic pressure
P	period of oscillation
$T_{1/2}$	time for oscillation to damp to one-half amplitude
$C_{m_\alpha} = \frac{\partial C_m}{\partial \alpha}$	
K	summation of aerodynamic derivatives contributing to moment caused by pitching velocity of body
$\mu$	relative density factor, $\frac{\text{Mass}}{\rho \text{ Volume}}$
$K_y$	nondimensional radius of gyration corresponding to $I_y$ , $k_y/L$
D	differential operator, $\frac{d}{ds}$
s	nondimensional time parameter based on length, $Vt/L$

$k_y$	radius of gyration corresponding to $I_y$
$t$	time
$\rho$	mass density of air
$\theta$	angle between tangent to body contour and longitudinal body axis in plane of symmetry in which $\alpha$ is measured
$dF$	force on element (positive when upward along transverse axis or rearward along longitudinal axis)
$dM$	pitching moment about center of gravity due to force on element (positive when sense of moment is nose up)
$x_m$	axial distance from bow of body to center of gravity
$r_e$	moment-arm distance (in plane perpendicular to longitudinal body axis) from the axis to center of gravity of projection of surface area of half the hollow cylinder element (used $\frac{2}{\pi}r$ , the value for a semicircumference, representing half of an infinitely thin hollow cylinder); see fig. 2
$C_m$	pitching-moment coefficient, $\frac{M}{q \text{ Volume}}$
$M$	pitching moment about center of gravity due to integration of forces on all body elements (positive when sense of moment is nose-up)
$c_{d\alpha=0^\circ}$	local longitudinal-force coefficient at an angle of attack of $0^\circ$ at any x-station based on body circumference
$c_{d\alpha=90^\circ}$	local transverse-force coefficient at an angle of attack of $90^\circ$ at any x-station based on body diameter
$c_{dc}$	circular-cylinder-section drag coefficient based on cylinder diameter
$\eta$	ratio of the drag coefficient of circular cylinder of finite length to that for cylinder of infinite length

## Subscripts:

t	transverse direction (perpendicular to longitudinal body axis)
l	longitudinal direction (parallel to longitudinal body axis)
av	average

## MODEL AND APPARATUS

## Model

Profile sketches and over-all dimensions of the bodies of revolution used in the investigation are presented in figure 1. The ordinates of the bodies are presented in table I. As can be seen in figure 1, the bodies included a hemisphere, a near-paraboloid, and four intermediate bodies. The six bodies shall sometimes be referred to in the remainder of this paper as bodies A through F, by which letters they are identified in figure 1 and table I. Each body of revolution was symmetrical about its longitudinal axis. For the experimental part of the investigation, the bodies used were made homogeneously of balsa segments and had lacquered surfaces. Mass and design information for the bodies are presented in table II, the center-of-gravity locations as listed in the table being the natural ones for the respective homogeneous bodies.

## Wind Tunnel

The Langley 20-foot free-spinning tunnel, which has an airspeed range up to about 95 feet per second, was used for the wind-tunnel test phase of the investigation. This tunnel has a vertically rising air stream and was convenient to use in investigating experimentally the behavior in descent of the bodies of revolution.

## EXPERIMENTAL TESTS

## Free-Drop Test Methods

In the free-drop tests, each body was held with its longitudinal axis in an attitude somewhere between vertical and an angle of attack of about  $20^\circ$  and was released to float in the tunnel air stream. Visual observations were made of the behavior of the body in the tunnel air stream. Descent velocity was recorded as the airspeed necessary to hold the body at a given level in the tunnel. For those bodies which descended

in a nose-down vertical attitude, the drag coefficient of the body at an angle of attack of  $0^\circ$  was obtained by dividing the weight of the body by the free-stream dynamic pressure at descent velocity and by the projected area of the body in a plane perpendicular to the longitudinal body axis. The results were analyzed to determine the effects of varying the body shape on the behavior of the bodies in descent. Reynolds numbers of the free-drop tests, based on lengths of the longitudinal axes and on the rates of descent of the bodies, ranged from about  $2.5 \times 10^4$  to about  $7.5 \times 10^4$ . Reynolds numbers based on cross-body components of velocity ( $V \sin \alpha$ ) and on body diameters at various stations along the longitudinal axis were for the most part between  $1.0 \times 10^4$  and  $3.0 \times 10^4$ , although the lower limit naturally approached zero for forward body stations with very small diameters or when the angle of attack of a body was very small.

### Free-Drop Test Results

The results of the free-drop tests are presented in table III. After being released to float in the tunnel air stream, the hemispherical and near-hemispherical bodies of revolution, bodies A and B in figure 1, quickly assumed a nose-down vertical attitude with little or no horizontal travel in the tunnel. Bodies C and D also trimmed generally in a nose-down vertical attitude, although for body C there were occasional oscillations of the order of  $\pm 5^\circ$  from the vertical, approximately about a lateral axis through the center of gravity, and for body D, there was some slight horizontal travel in the tunnel. Body E trimmed in a nose-down vertical attitude part of the time but also tended to make erratic falling-leaf motions which eventually evolved to a continuous end-over-end tumbling motion approximately about a lateral body axis through the center of gravity while traveling horizontally in the tunnel. Body F, a near-paraboloid, descended with a tumbling motion similar to the one just described. The results indicated that the stability in descent of the homogeneous balsa bodies A to F decreased as the body shapes became less like that of a hemisphere. Although this decrease in stability may have been due in part to more rearward (percentagewise) center-of-gravity locations, a comparison of the stability of bodies C and F, which had identical center-of-gravity locations, indicates a definite effect of shape on stability. A brief additional test was made in which lead ballast was attached to the front of body F, causing the center of gravity to move forward far enough so that the body trimmed in a nose-down vertical attitude. If sufficient turning moment was applied at launching to start any of the bodies rotating, the body would descend in the tunnel with a tumbling motion similar to that described for body E. The causes and geometry of these tumbling motions are not considered in this paper, inasmuch as such a study is beyond the scope of the present investigation.

### Free-Oscillation Test Methods

As mentioned earlier, it was noticed during the free-drop tests that the motion of four of the subject bodies of revolution (A, B, C, and F with its center of gravity moved forward) as they floated in the air stream of the wind tunnel appeared to be substantially a single-degree-of-freedom motion approximately about a lateral axis through the center of gravity of the body. Based on the assumption that such a motion was present, motion pictures were made as the bodies were forced to oscillate by means of an externally applied moment, and the period of the oscillations and the time to damp to one-half amplitude were obtained from the film records. By using the values of  $P$  and  $T_{1/2}$ , values of  $C_{m\alpha}$ , as well as of  $K$  (representing the summation of the derivatives contributing to the moment caused by the pitching velocity of the body), were determined as shown in the appendix.

### Free-Oscillation Test Results

The values of  $K$  and  $C_{m\alpha}$  obtained for the four bodies from oscillation during the free drop are listed in table IV. As illustrated for body B in the appendix, the term containing  $K$  in the root of the equation of motion when applied to each of the bodies was found to be so small that it had only a negligible effect on the values of  $C_{m\alpha}$  (static stability) obtained. The degrees of static stability of the various bodies as determined from the free-oscillation tests showed qualitative agreement with the relative degrees of stability indicated by the motions observed during the free-drop tests.

## STABILITY CALCULATIONS

### Method of Calculating Stability

As air flows around a body of revolution of the subject type when inclined at an angle of attack, the velocities over the bottom surface are different from those on the top half, and these velocity differences cause unbalanced pressures and forces which may cause a pitching moment on the body. An attempt is made here to develop a convenient method for estimating the pitching moments of the bodies without the necessity of making a detailed study of pressures and forces at various points on the front or base surfaces. Consideration is given, by a strip-analysis method, to forces on the body normal to the surface profile in the plane of symmetry in which  $\alpha$  is measured, the forces being taken as functions of the free-stream velocity components in that normal direction. In using this approach, cognizance was taken of some two-dimensional results presented in reference 3 which indicate that the force on a circular cylinder

in the defined normal direction is a function of the component of free-stream velocity in that direction. The (frictional) flow parallel to the surface profile is disregarded.

It is convenient to consider a body element of length  $dx$  (see fig. 2) as being the wedge-shaped front of a hollow right-circular-cylinder element with a length of  $L - x$ , a thickness of  $dr$ , and projected surface areas in longitudinal and transverse (parallel and perpendicular, respectively, to longitudinal body axis) body planes of  $2r dx$  and  $2\pi r dr$ . When the body of revolution is at an angle of attack, the components of free-stream velocity normal to the surface at the bottom and top points of the body element  $dx$  in the plane in which  $\alpha$  is measured may be expressed, respectively, as  $V \sin(\theta + \alpha)$  and  $V \sin(\theta - \alpha)$ . On the base of the body (rear surface of the hollow cylinder) directly behind the bottom and top points on the front, the free-stream velocity components normal to the surface may each be expressed as  $V \cos \alpha$ . For convenience, let us consider the unbalanced force on the hollow-cylinder element due to these different normal velocity components in terms of separate transverse and longitudinal forces. At the bottom and top points, respectively, of the front of the element, the transverse force components would be proportional to

$$\frac{\rho}{2} V^2 \sin^2(\theta + \alpha) \cos \theta$$

and

$$\frac{\rho}{2} V^2 \sin^2(\theta - \alpha) \cos \theta$$

and the longitudinal force components would be proportional to

$$\frac{\rho}{2} V^2 \sin^2(\theta + \alpha) \sin \theta$$

and

$$\frac{\rho}{2} V^2 \sin^2(\theta - \alpha) \sin \theta$$

(vectors shown in fig. 2). On the rear surface of the hollow cylinder there would be no transverse force components and the longitudinal force components at both the bottom and top points of the element would be proportional to  $\frac{\rho}{2} V^2 \cos^2 \alpha$ . The pitching moment about the center of gravity of the body due to the transverse and longitudinal forces on the element is

$$dM = dF_t(x_m - x) + dF_l r_e \quad (1)$$

Expanding equation (1) by use of the foregoing relationships, and including the local force coefficients  $c_{d_{\alpha=90^\circ}}$  and  $c_{d_{\alpha=0^\circ}}$  gives

$$\begin{aligned} dM = & c_{d_{\alpha=90^\circ}} \left[ q \sin^2(\theta + \alpha) \cos \theta - q \sin^2(\theta - \alpha) \cos \theta \right] (x_m - x) 2r \, dx - \\ & c_{d_{\alpha=0^\circ}} \left[ q \sin^2(\theta + \alpha) \sin \theta - q \cos^2 \alpha \right] 2r_e \pi r \, dr + \\ & c_{d_{\alpha=0^\circ}} \left[ q \sin^2(\theta - \alpha) \sin \theta - q \cos^2 \alpha \right] 2r_e \pi r \, dr \end{aligned}$$

or

$$\begin{aligned} dM = & 2q c_{d_{\alpha=90^\circ}} \cos \theta \left[ \sin^2(\theta + \alpha) - \sin^2(\theta - \alpha) \right] (x_m - x) r \, dx - \\ & 2\pi q c_{d_{\alpha=0^\circ}} \sin \theta \left[ \sin^2(\theta + \alpha) - \sin^2(\theta - \alpha) \right] r_e r \, dr \end{aligned}$$

It can be shown by expanding and collecting terms that

$$\left[ \sin^2(\theta + \alpha) - \sin^2(\theta - \alpha) \right] = \sin 2\alpha \sin 2\theta$$

and, since  $r_e = \frac{2r}{\pi}$ ,

$$\begin{aligned} dM = & 2q \sin 2\alpha c_{d_{\alpha=90^\circ}} \cos \theta \sin 2\theta (x_m - x) r \, dx - \\ & 4q \sin 2\alpha c_{d_{\alpha=0^\circ}} \sin \theta \sin 2\theta r^2 dr \end{aligned} \quad (2)$$

The moment due to the forces over the whole body may be obtained by integrating the incremental moments over the length of the body.

In the present investigation, the value of  $C_{D_{\alpha=0^\circ}}$  (table III) determined from the free-drop tests of each body was used as  $c_{d_{\alpha=0^\circ}}$  for all body elements of that particular body. In regard to values for  $c_{d_{\alpha=90^\circ}}$ , it was believed that the present purpose of calculating the

approximate stability of the bodies could be achieved by using the value of the product  $\eta c_{d_c} (\cos \theta)_{av}$  as  $c_{d_{\alpha=90^\circ}}$  for all body elements of a particular body. The quantity  $\eta c_{d_c}$  was originally intended (ref. 4) for use in determining the average section drag coefficient of a circular cylinder of finite length and the  $(\cos \theta)_{av}$  term is intended as an attempt to compensate for the fact that  $\eta c_{d_c}$  does not include the effects of body curvature along the length of the present bodies. Although values of  $\eta c_{d_c}$  were obtained (ref. 4) only at a cross-flow Reynolds number of  $8.8 \times 10^4$ , they are assumed herein to be applicable over the Reynolds number range of the present investigation, in which range  $c_{d_c}$  has a constant value of 1.2. A value of  $\eta$  was obtained for each body by extrapolating the curve shown in figure 3 which is based on the results of the aforementioned experiments on circular cylinders. A value of  $(\cos \theta)_{av}$  was obtained for each body by plotting a curve of  $\cos \theta$  against body station, integrating the area under the curve, and then dividing by the body length.

In the present investigation, integrations of the products of the variables in the two terms of equation (2) were performed graphically and multiplied by the respective factors  $\frac{2 \sin 2\alpha c_{d_{\alpha=90^\circ}}}{\text{Volume}}$  and  $\frac{4 \sin 2\alpha c_{d_{\alpha=0^\circ}}}{\text{Volume}}$  for an angle-of-attack range from  $0^\circ$  to  $90^\circ$  to obtain the pitching-moment coefficient over this range.

### Results of Stability Calculations

The results of the calculations are presented in figure 4 and in the tabulated values of  $C_{m_\alpha}$  in table V. As would be expected from the nature of the equation used in calculating the pitching moment, the curves for  $C_m$  against  $\alpha$  are symmetrical about a maximum value at an angle of attack of  $45^\circ$  and return to a value of zero at an angle of attack of  $90^\circ$ . The results indicate that all the bodies except body F are statically stable, and the results are therefore in qualitative agreement with the wind-tunnel test results discussed earlier in this paper. For the various statically stable bodies, the slopes of the curves show a general agreement between the relative degrees of stability as obtained experimentally and as calculated; that is, bodies A and B are most stable, body C less stable, and so forth. Good quantitative agreement was obtained between the  $C_{m_\alpha}$  values from the calculation method and those obtained from the oscillation techniques, as may be seen by comparing

tables IV and V. It is of interest that the results of the calculations for body F with its center of gravity moved forward to 50-percent body length indicate stability; this result is in agreement with the experimental results. Table V includes a breakdown of the calculated resultant stability of each body in terms of the contributions to  $C_{m\alpha}$  caused by the respective transverse and longitudinal forces. As can be seen from the table, the contributions due to the longitudinal force for each body was a stabilizing moment, whereas the contribution due to the transverse force was destabilizing except for body F with its center of gravity moved forward.

It is of interest that, if an average value of  $cd_{\alpha=0}$  based on the six measured values obtained for the bodies of the present investigation had been used in calculating the stability of each body, the changes in  $C_{m\alpha}$  would be within about  $\pm 20$  percent of the values calculated. Thus, it appears that, if the method developed for calculating the stability of the subject bodies is applied to other bodies of the same general type and no measured value of  $cd_{\alpha=0}$  is available, an average or estimated value of  $cd_{\alpha=0}$  can be used and should allow qualitative determination of the stability of the body with a reasonable degree of reliability.

#### CONCLUDING REMARKS

An investigation has been made of the stability of several bodies of revolution having fineness ratios smaller than 1.0 and having rounded fronts and blunt bases. Free-drop tests were made in the vertical Langley 20-foot free-spinning tunnel to determine the behavior of the various bodies in descent. The results indicated that the stability of the bodies as determined from observed motions decreased as the body shapes varied from a hemisphere to a near-paraboloid. Free-oscillation tests were made for some of the bodies and the static stability parameter  $C_{m\alpha}$  was found to be indicative of the relative behaviors noted during the free-drop tests. In addition to the determination of stability from the free-body tests, a method for calculating the approximate stability of the subject type of body was developed. Results obtained by this calculation method agreed well with the experimental results.

Langley Aeronautical Laboratory,  
National Advisory Committee for Aeronautics,  
Langley Field, Va.

## APPENDIX

## METHOD OF DETERMINING STABILITY OF BODY BY OSCILLATION TECHNIQUE

The applicable nondimensional single-degree-of-freedom equation of motion for the bodies of revolution is

$$2\mu K_Y^2 D^2 \alpha - \frac{K}{2} D \alpha - C_{m\alpha} \alpha = 0$$

from which the characteristic equation is

$$2\mu K_Y^2 D^2 - \frac{K}{2} D - C_{m\alpha} = 0$$

or

$$D^2 - \frac{K}{4\mu K_Y^2} D - \frac{C_{m\alpha}}{2\mu K_Y^2} = 0$$

The roots are

$$D = \frac{K}{8\mu K_Y^2} \pm \sqrt{\left(\frac{K}{8\mu K_Y^2}\right)^2 + \frac{C_{m\alpha}}{2\mu K_Y^2}}$$

The formulas

$$T_{1/2} = \frac{0.693}{\text{Real part of root}} \frac{L}{V}$$

and

$$P = \frac{2\pi}{\text{Imaginary part of root}} \frac{L}{V}$$

were used to determine  $K$  and  $C_{m\alpha}$ . In order to illustrate the use of this technique, work done for body B is shown. From an extrapolation of the plot in figure 5, which was prepared from motion-picture records of the oscillations of body B, it was determined that

$$T_{1/2} = 1.17 \text{ sec}$$

Then, into the formula

$$T = 1.17 \text{ sec} = \frac{0.693 \left( 8\mu K_Y^2 \right)}{K} \frac{L}{V}$$

the following constant values for body B are substituted

$$L = 0.1475 \text{ ft}$$

$$V = 46.5 \text{ ft/sec}$$

$$\mu = 146.8$$

$$K_Y^2 = 0.1953$$

Therefore,

$$K = -0.4305$$

where the negative sign is inserted with the quantitative value of  $K$  because the damping opposes the oscillatory motion.

From figure 5, it was also determined that

$$P = 0.35 \text{ sec}$$

Then, from the formula

$$P = 0.35 = \frac{2\pi}{\sqrt{\left( \frac{K}{8\mu K_Y^2} \right)^2 + \frac{C_{m\alpha}}{2\mu K_Y^2}}} \frac{L}{V}$$

and by using the constants and  $K$  for body B it was found that

$$C_{m\alpha} = -0.186$$

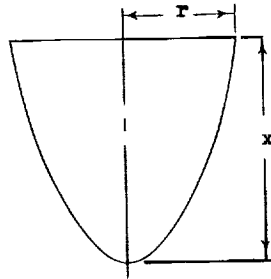
where the minus sign is inserted with the quantitative value of  $C_{m\alpha}$  because the static stability opposes the oscillatory motion.

## REFERENCES

1. Munk, Max M.: The Aerodynamic Forces on Airship Hulls. NACA Rep. 184, 1924.
2. Allen, H. Julian, and Perkins, Edward W.: A Study of Effects of Viscosity on Flow Over Slender Inclined Bodies of Revolution. NACA Rep. 1048, 1951. (Supersedes NACA TN 2044.)
3. Jones, Robert T.: Effects of Sweepback on Boundary Layer and Separation. NACA Rep. 884, 1947. (Supersedes NACA TN 1402.)
4. Fluid Motion Panel of the Aeronautical Research Committee and Others: Modern Developments in Fluid Dynamics. Vol. II, ch. 9, sec. 195, S. Goldstein, ed., The Clarendon Press (Oxford), 1938.

TABLE I.- ORDINATES FOR BODIES OF REVOLUTION TESTED IN THE

LANGLEY 20-FOOT FREE-SPINNING TUNNEL

[Values for  $r$  and  $x$  are in inches]

Body A	
Hemisphere Radius, 1.25 inches	

Body B	
$r$	$x$
0	0
.426	.084
.600	.169
.840	.338
1.015	.507
1.15	.676
1.238	.845
1.33	1.014
1.373	1.184
1.427	1.353
1.461	1.522
1.475	1.691
1.488	1.772

Body C	
$r$	$x$
0	0
.342	.097
.519	.195
.740	.389
.900	.584
1.030	.778
1.130	1.000
1.218	1.168
1.280	1.362
1.360	1.560
1.430	1.750
1.490	1.945
1.515	2.040

Body D	
$r$	$x$
0	0
.373	.097
.521	.194
.746	.388
.886	.583
1.003	.777
1.112	.972
1.197	1.166
1.244	1.360
1.298	1.555
1.345	1.749
1.368	1.944
1.384	2.037

Body E	
$r$	$x$
0	0
.322	.108
.488	.216
.695	.433
.840	.650
.965	.865
1.060	1.070
1.142	1.299
1.205	1.515
1.277	1.730
1.340	1.950
1.400	2.160
1.422	2.270

Body F	
$r$	$x$
0	0
.310	.125
.470	.250
.670	.500
.810	.750
.930	1.000
1.000	1.250
1.100	1.500
1.160	1.750
1.230	2.000
1.280	2.250
1.350	2.500
1.370	2.620



TABLE II.-- DIMENSIONAL AND MASS DATA FOR BODIES OF REVOLUTION  
TESTED IN THE LANGLEY 20-FOOT FREE-SPINNING TUNNEL

Body	Fineness ratio	Length, ft	Volume, ft <sup>3</sup>	Weight, lb	Center-of-gravity location, percent length	Moment of inertia, I <sub>y</sub> , slug-ft <sup>2</sup>
A	0.5	0.1042	0.002365	0.02315	59.6	0.1989 × 10 <sup>-5</sup>
B	.595	.1475	.00451	.0507	60.9	.669
C	.673	.170	.004669	.0573	64.0	.790
D	.736	.1697	.00428	.0468	61.4	.606
E	.798	.1892	.00456	.0601	64.5	.837
F	.956	.218	.00477	.0463	64.0	.742
a <sub>F</sub>	.956	.218	.00477	.0585	50.0	1.40

<sup>a</sup>Lead ballast added to front of body F to move center of gravity forward.



TABLE III.- RESULTS OF EXPERIMENTAL TESTS OF BODIES OF REVOLUTION  
IN THE LANGLEY 20-FOOT FREE-SPINNING TUNNEL

Body	V (rate of descent when in nose vertically down attitude), fps	$C_{D_{\alpha=0^\circ}}$	Behavior of body in descent
A	39.8	0.362	Trimmed in nose vertically down attitude; no horizontal travel in tunnel.
B	46.5	.410	Trimmed in nose vertically down attitude; no horizontal travel in tunnel.
C	49.0	.402	Trimmed generally in nose vertically down attitude; made occasional oscillations of $\pm 50^\circ$
D	51.0	.363	Trimmed generally in nose vertically down attitude; traveled horizontally in tunnel very slowly.
E	53.0	.408	Trimmed generally in nose vertically down attitude; made occasional oscillations of $\pm 50^\circ$ and traveled horizontally in tunnel very slowly; sometimes tumbled while traveling horizontally in tunnel.
F	<sup>a</sup> 50.0	.382	Tumbled and traveled horizontally in tunnel.
bF	<sup>b</sup> 53.0	<sup>b</sup> .429	Trimmed in nose vertically down attitude; no horizontal travel in tunnel.

<sup>a</sup>Estimated value if model had descended in nose vertically down attitude.

<sup>b</sup>Lead ballast added to front of body F to move center of gravity forward.




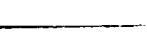

TABLE IV.- VALUES OF  $K$  AND  $C_{m\alpha}$  OBTAINED FROM OSCILLATION TECHNIQUE

Body	$K$	$C_{m\alpha}$ per radian
A	1.242	-0.272
B	.430	-.186
C	1.21	-.128
<sup>a</sup> F	1.38	-.149



<sup>a</sup>Center of gravity of body F moved forward to 50-percent body length.

TABLE V.- CALCULATED VALUES OF  $C_{m\alpha}$  AND BREAKDOWN INDICATING RELATIVE CONTRIBUTIONS OF TRANSVERSE AND LONGITUDINAL FORCES TO  $C_{m\alpha}$ .

Body	$C_{m\alpha}$ per radian (from slope of calculated curves in fig. 4)	Component of $C_{m\alpha}$ due to transverse forces		Component of $C_{m\alpha}$ due to longitudinal forces	
		Sense	Magnitude in percentage of value of $C_{m\alpha}$ (a)	Sense	Magnitude in percentage of value of $C_{m\alpha}$ (a)
A	-0.250	 Destabilizing	12	 Stabilizing	112
B	-.162		30		130
C	-.118		39		139
D	-.064		93		193
E	-.050		142		242
F	+0.010	 Stabilizing	889		789
<sup>b</sup> F	-.132		32		68



<sup>a</sup>Sum of two percentages is 100 percent.

<sup>b</sup>Center of gravity of body F moved forward to 50-percent body length.

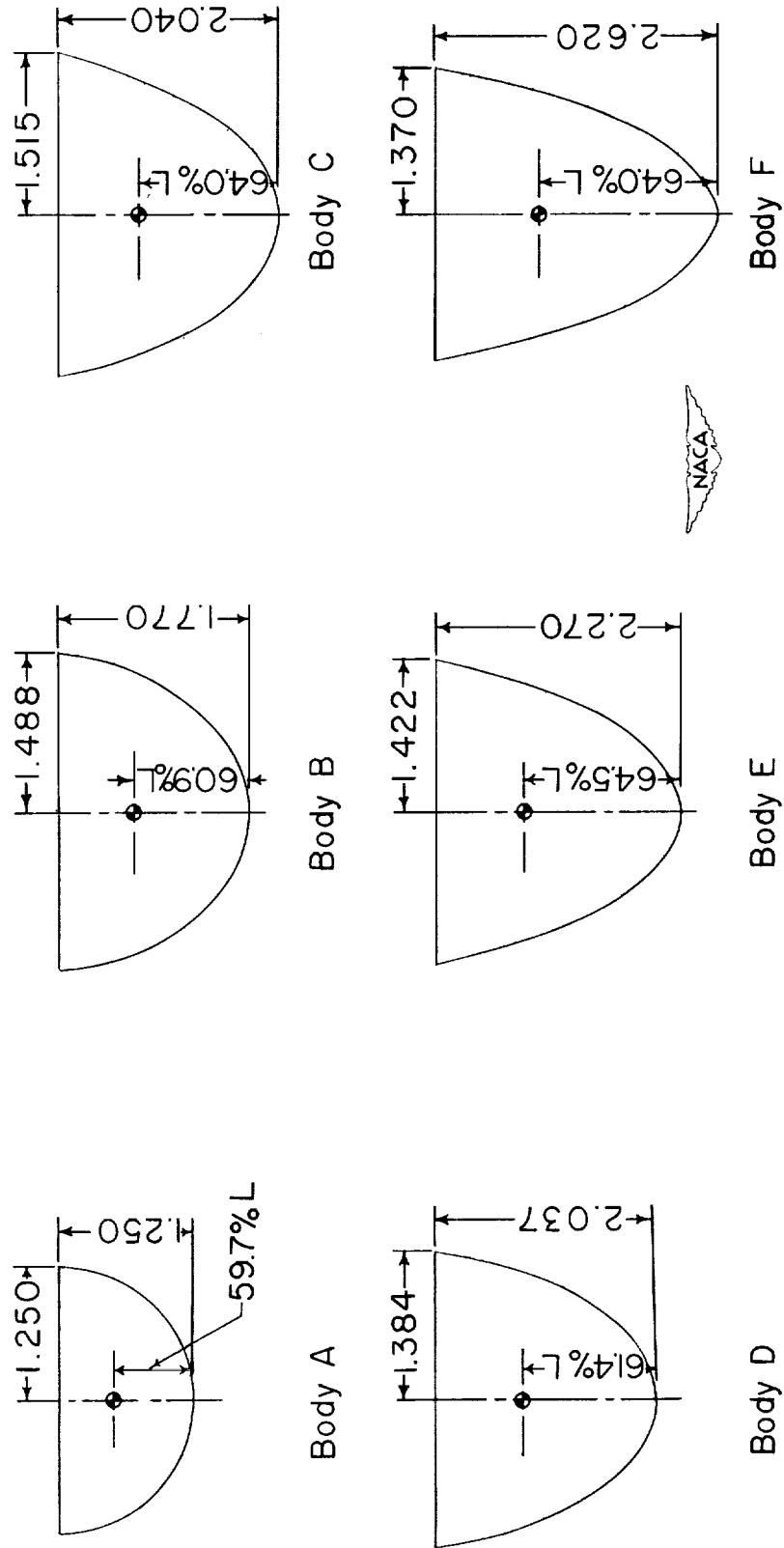


Figure 1.- Profile sketches of bodies of revolution tested in the Langley 20-foot free-spinning tunnel. All dimensions are in inches.

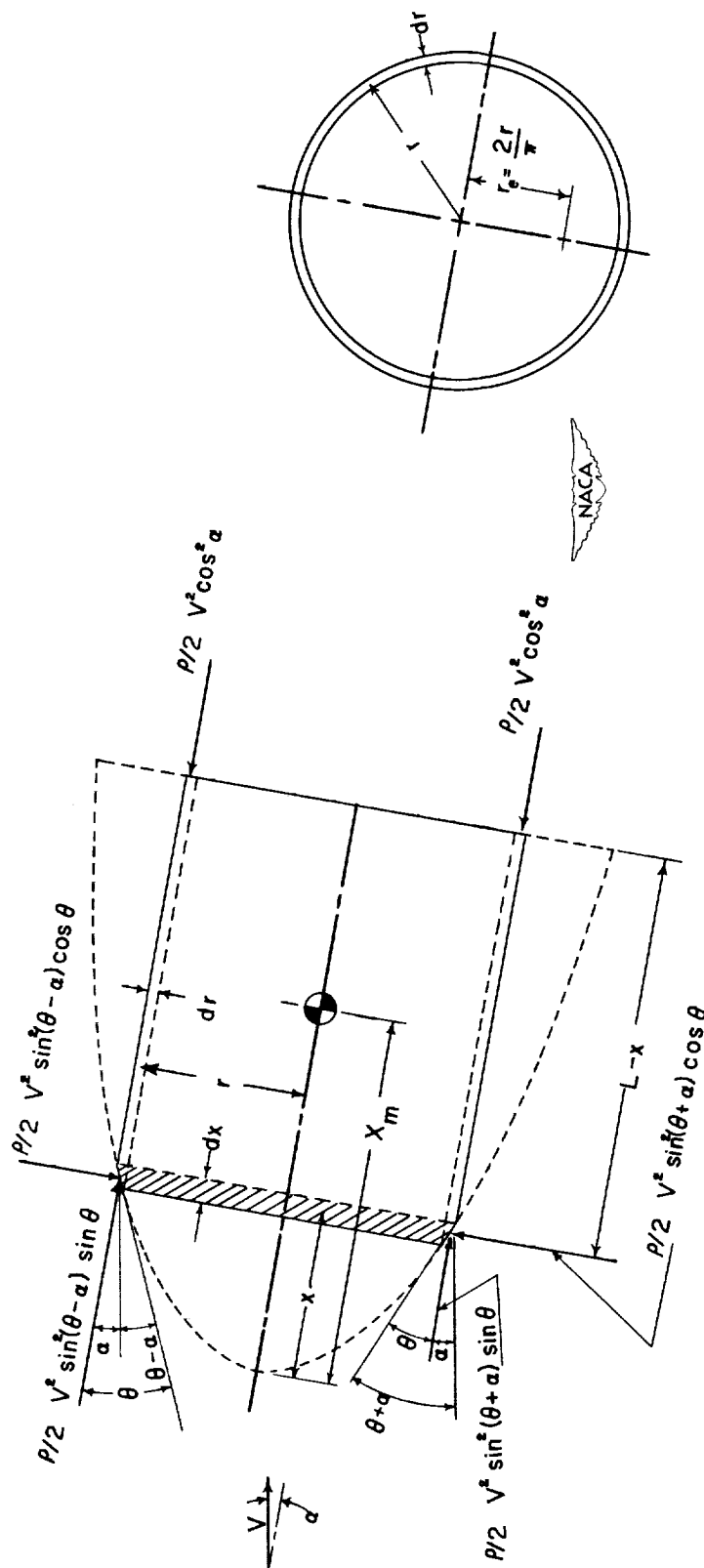


Figure 2.- Sketch showing geometry of body element and directions of force-proportionality vectors.

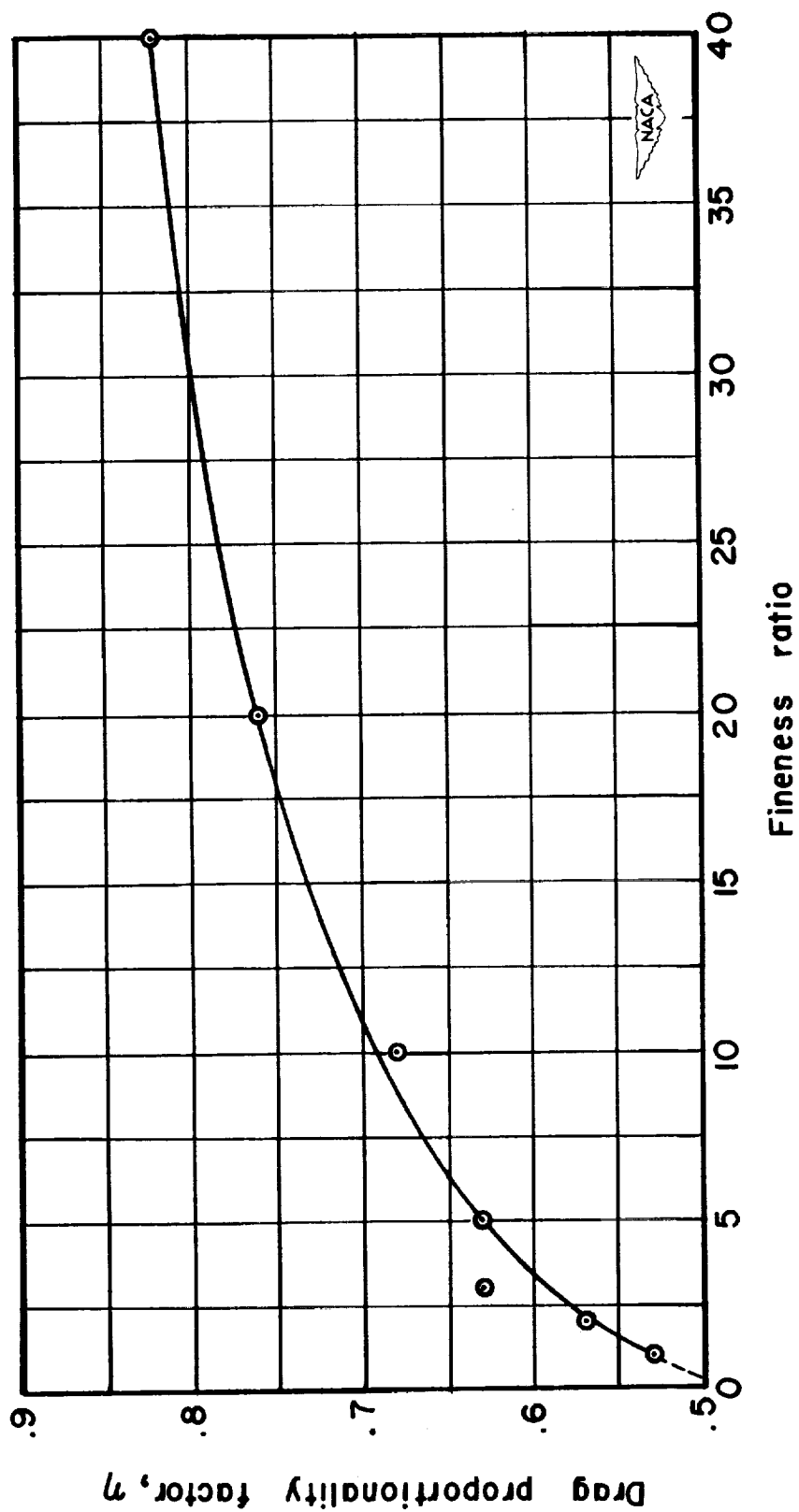


Figure 3.- Ratio of the drag coefficient of a circular cylinder of finite length to that of a cylinder of infinite length as a function of the fineness ratio. Data taken from reference 4. Reynolds number,  $8.8 \times 10^4$ .

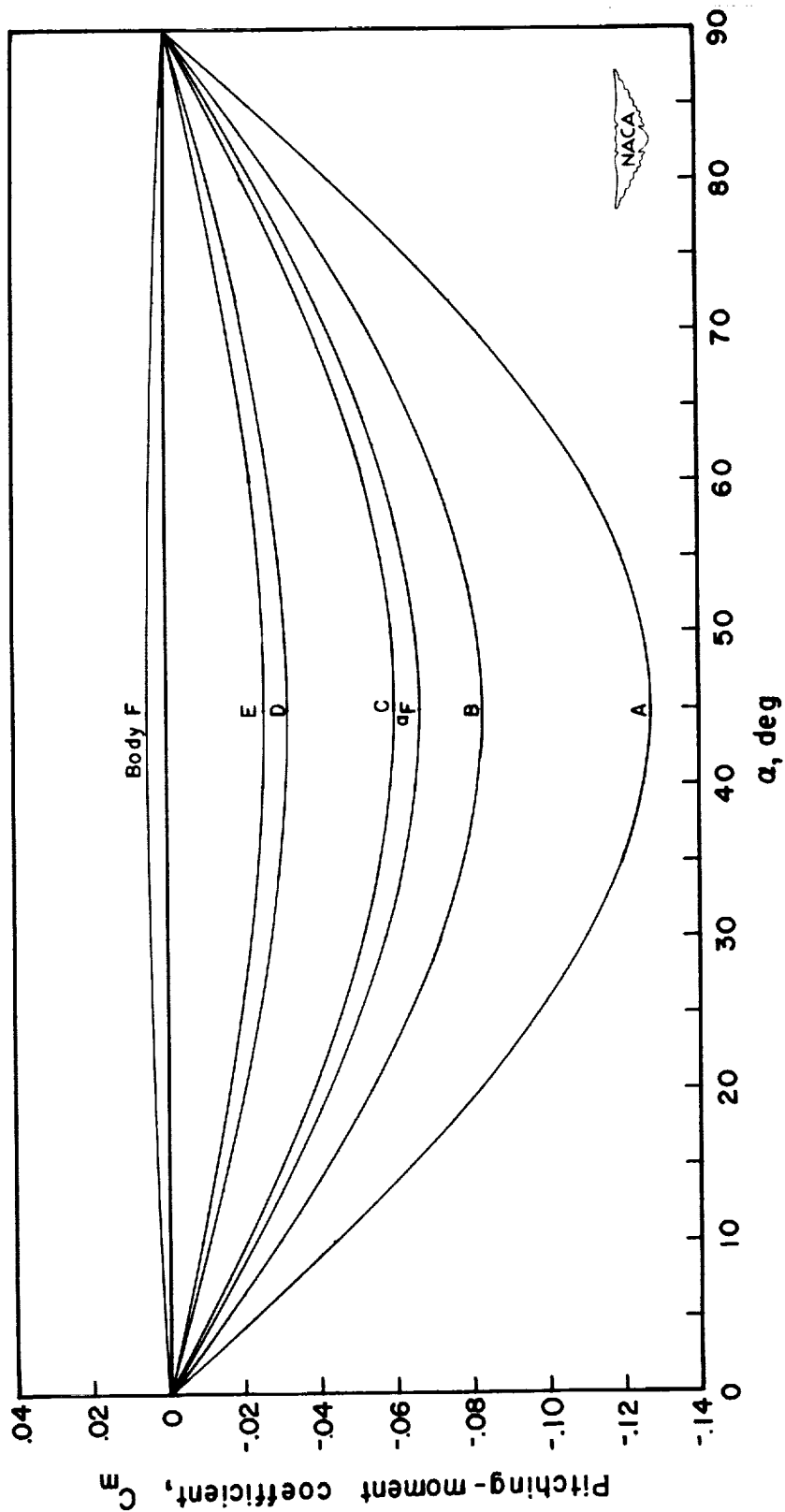


Figure 4.- Calculated curves for  $C_m$  against  $\alpha$  for bodies of revolution.  
For description of bodies, see table II.

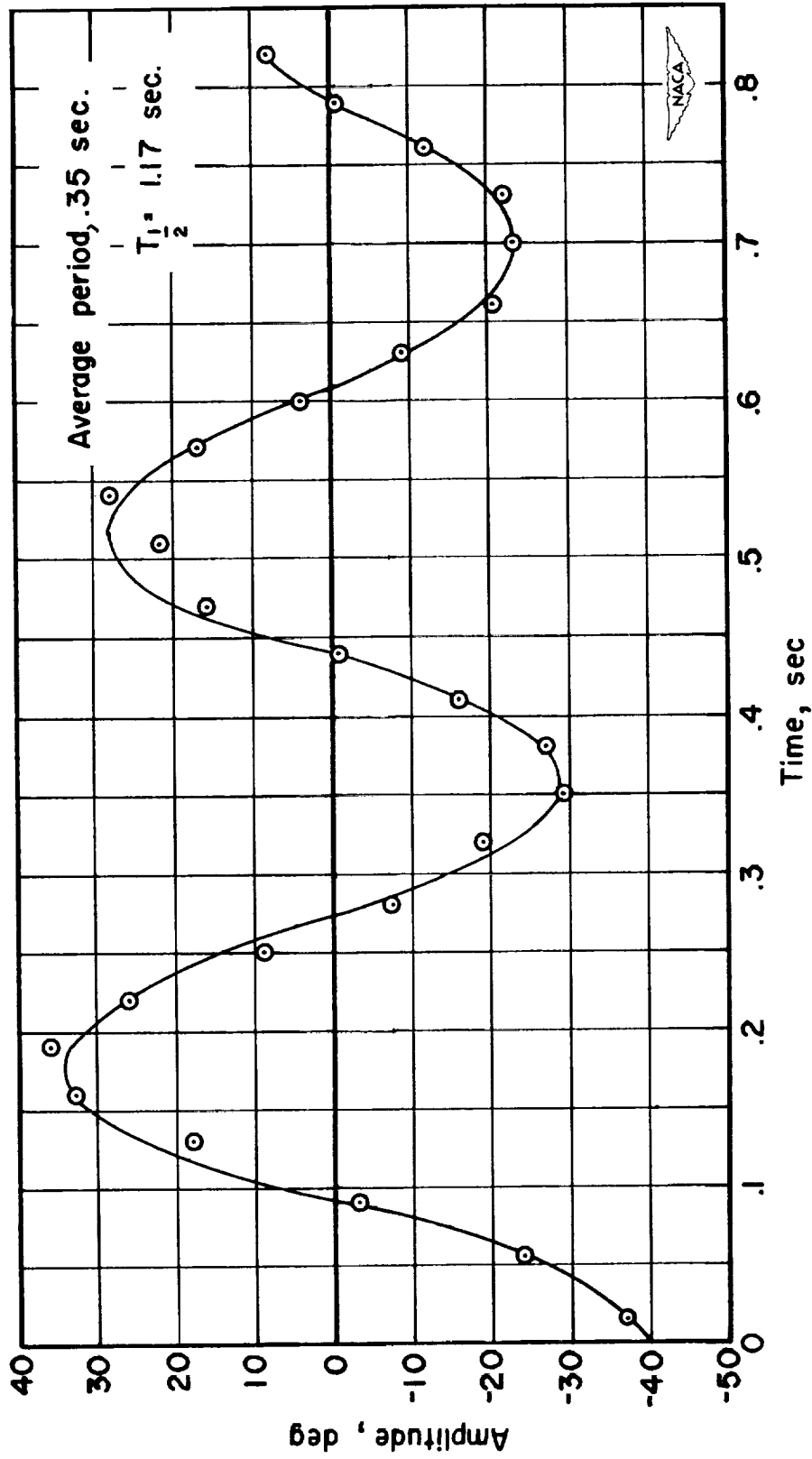


Figure 5.- Variation of amplitude of oscillation with time for body B as obtained from motion-picture records.

•

•

•

•

•

•